Iranian Journal of Fuzzy Systems
Volume 23, Number 6, (2026), pp. 189-207
Original paper

Multivariable fuzzy PID controller using convex optimization and positive real lemma for nonlinear systems

M. Ataie[1] and M. Edrisi[2]

[1,2] *Department of Electrical Engineering, Isfahan University, Isfahan, Iran*

ataiemilad41@gmail.com, edrisi@eng.ui.ac.ir

Abstract

In this study, an algorithm is proposed for the design of a multivariable fuzzy PID controller using convex optimization and linear matrix inequality (LMI) constraints. The considered fuzzy system is of the Takagi–Sugeno type and consists of subsystems based on PID controllers. The parameters of these subsystems are optimized to achieve desirable performance. The positive real lemma is employed to guarantee the stability of the overall fuzzy system. One of the most significant applications of this approach lies in the control of industrial robots. Since robotic systems are typically multivariable in nature, the utilization of advanced controllers such as multivariable fuzzy PID controllers can play a crucial role in enhancing their performance. In this work, the proposed control scheme will be implemented both on a simulation example and a practical robot manipulator.

Keywords: Proportional, derivative, integral controller, fuzzy logic, MIMO fuzzy PID, multivariable system, robot manipulator, convex optimization based LMI, positive real systems.

1 Introduction

Robotic manipulators have experienced significant advancements in recent years due to their wide range of applications in industrial automation, medical systems, military operations, and hazardous or toxic environments. A major motivation for employing industrial robots is cost reduction. Studies have indicated that, since the 1990s, the cost of robotic systems has decreased, while human labor costs have steadily increased. In addition to their economic advantages, robots have become faster, more accurate, and increasingly flexible in operation [22]. Given their inherently nonlinear and multivariable dynamics, robotic systems present significant challenges in control design. Among the various control strategies, the Proportional-Integral-Derivative (PID) controller remains one of the most widely used methods in industrial practice, owing to its simplicity, fast transient response, acceptable steady-state performance, and ease of implementation [3]. However, for complex systems-such as those with high-order dynamics, time delays, or oscillatory behavior-the conventional PID controller may not provide satisfactory performance. In such cases, fuzzy controllers offer a viable alternative by accommodating system nonlinearities more effectively. Classical control design approaches such as pole placement, optimal control, and frequency response methods are generally applicable only to linear systems. In contrast, fuzzy control techniques, being inherently nonlinear, can address a broader range of problems [21]. The integration of fuzzy logic with PID control has led to the development of fuzzy PID controllers, which aim to combine the intuitive rule-based framework of fuzzy logic with the well-established performance of PID controllers. Since the performance of PID control is highly sensitive to parameter tuning [18], designing a fuzzy PID controller for multivariable systems becomes a complex optimization problem involving multiple parameters. For a system with m inputs and n outputs, the PID controller requires tuning of 3mn parameters, corresponding to the proportional, integral, and

Corresponding Author: M. Ataie
Received: October 2025; Revised: June 2026; Accepted: September 2026.
https://doi.org/10.22111/ijfs.2026.53636.9494

derivative matrix gains. For example, a 2-input 2-output (2×2) system requires 12 parameters, while a 4×4 system necessitates tuning 48 parameters. The same parameter complexity applies to multivariable fuzzy PID (MFP)controllers, where each local subsystem must be tuned individually. Recent advances in convex optimization and Linear Matrix Inequality (LMI) theory have significantly reshaped the landscape of multivariable and robotic control systems, offering robust frameworks for addressing the complexities of multi-input multi-output (MIMO) dynamics and nonlinearities. A particularly active area of research has been the integration of fuzzy logic with convex optimization, leading to powerful methodologies for controller design. Within the Takagi-Sugeno (TS) fuzzy framework, which naturally handles nonlinear systems through a convex combination of local linear models, significant progress has been made in developing less conservative LMI conditions for stabilization [16]. Notably, an improved Parallel Distributed Compensation (PDC) law has been proposed that explicitly incorporates the time derivatives of membership functions into the control structure, embedding a form of anticipatory behavior that reduces conservatism and enlarges the domain of attraction. This advancement builds directly upon Fuzzy Lyapunov Function (FLF) theory, where stability conditions are expressed as solvable LMIs. In parallel, fuzzy PID controllers have been successfully developed for complex infinite-dimensional systems, such as nonlinear parabolic partial differential equations (PDEs), where a TS fuzzy PDE model is constructed and a fuzzy PID boundary output tracking control law is synthesized, with parameter tuning formulated directly as an LMI feasibility problem [25]. The effectiveness of such fuzzy PID schemes has been demonstrated on benchmark examples including chemical axial dispersion tubular reactors, where they exhibit faster response and reduced overshoot compared to fuzzy PI or fuzzy integral controllers. For general continuous-time TS fuzzy systems, output-feedback control design via homogeneous polynomial Lyapunov functions has been shown to provide less conservative stabilization conditions than traditional quadratic approaches, particularly when the bounds on membership function derivatives are unknown [17]. The theoretical foundations of LMIs in fuzzy control have also been extended to address practical implementation challenges, including robust dynamic output feedback under inexact premise variable measurements, where additive uncertainties in membership functions are explicitly modeled within the LMI framework [13]. On the experimental front, robust fuzzy control based on TS models has been validated on challenging mechanical systems such as the two-degree-of-freedom ball balancer, successfully incorporating constraints on control signal saturation, decay rate, and position feedback [24]. The integration of convex optimization with PID structures extends beyond traditional control synthesis; for instance, zeroing neural networks with proportional-integral-parameter adaptive convergence have been developed to solve quaternion-valued time-varying linear matrix inequalities, demonstrating both efficiency and intelligence in numerical optimization [15]. Furthermore, while recent LMI-based methods have been developed for robust multivariable PID design for MIMO second-order systems, successfully validated on experimental mobile inverted pendulum robots [9], and linear programming frameworks have been established for continuous-time positive systems to address the derivative-component challenges inherent in PID control [12]. Collectively, these developments from 2024 onwards highlight a definitive shift towards employing convex, LMI-based frameworks as a powerful and unifying methodology for the design, analysis, and experimental validation of advanced fuzzy, multivariable, and robotic control systems. Conventional PID controllers, when designed based on linearized robot models, typically perform well only within a limited region of the workspace. In contrast, the proposed T–S fuzzy PID controller can cover a broader operational range using only a few local linear subsystems. Furthermore, it demonstrates robustness to uncertainties and external disturbances. One of our practical implementations involves a 5-degree-of-freedom Mentor robotic arm, where the system parameters such as link masses are assumed to be unknown. Despite these uncertainties, the proposed fuzzy PID controller successfully regulates the robotic motion, confirming its effectiveness in real-world scenarios. The paper is organized such that Section 2 presents a brief yet comprehensive review of nonlinear systems, after which the Jacobian linearization technique is discussed, and the transfer function of multivariable systems is examined. Section 3 is dedicated to controller design. In this section, the general optimization framework for a multivariable PID controller for an LTI system is established. Subsequently, we show how this problem can be extended to a multivariable fuzzy PID system, and this extension is investigated using the positive real lemma. Section 4 evaluates the performance of the designed controller via simulations and practical case studies.

2 Problem formulation

2.1 Nonlinear systems

A general nonlinear multivariable system can be described by the following state-space equation:

$$\dot{x}(t) = f(x(t), u(t)), \tag{1}$$

where $\dot{x} \in \mathbb{R}^n$ denotes the time derivative of the state vector $x \in \mathbb{R}^n$, $u \in \mathbb{R}^m$ is the control input, and $f : \mathbb{R}^n \times \mathbb{R}^m \to \mathbb{R}^n$

is a nonlinear vector-valued function of the states and control inputs. The system output is given by:

$$y = h(t, x, u). \tag{2}$$

Equations (1) and (2) constitute the general nonlinear state-space representation of the system. To facilitate analysis and control design, it is common to recast (1) in an affine-in-control form:

$$\dot{x} = f(x) + g(x)u, \tag{3}$$

where $f(x)$ captures the autonomous dynamics and $g(x)$ represents the input coupling.

To design controllers using linear control theory, it is necessary to linearize the nonlinear system around a given operating point. Jacobian linearization provides a first-order approximation of the nonlinear dynamics. For the system described above, the linearized model near the equilibrium point (x_0, u_0) is given by[4]:

$$\begin{aligned} \dot{Z} &= AZ + Bv, \\ y &= CZ + Dv, \end{aligned} \tag{4}$$

where $Z = x - x_0$ and $v = u - u_0$ denote the perturbations from the equilibrium. The matrices A, B, C, and D are the Jacobians of f and h evaluated at the operating point. In the case of a linear time-invariant (LTI) multivariable system with m inputs and n outputs, the system's transfer function matrix is given by:

$$G(s) = C(sI - A)^{-1}B + D = \begin{bmatrix} g_{11}(s) & \cdots & g_{1m}(s) \\ \vdots & \ddots & \vdots \\ g_{n1}(s) & \cdots & g_{nm}(s) \end{bmatrix}. \tag{5}$$

In the matrix $G(s)$, the diagonal elements correspond to the transfer functions associated with each matched input-output pair, while the off-diagonal elements represent the transfer functions for cross-coupled or unmatched pairs, which are indicative of system interactions.

2.2 Notations:

For a complex matrix $F \in \mathbb{C}^{p\times q}$, the spectral norm of F, defined as the maximum singular value, is denoted by $\|F\|$. Consider a $p \times q$ transfer function matrix $H(s)$. Its H_∞-norm, denoted by $\|H\|_\infty$, is defined as the supremum of the spectral norm over the open right-half plane:

$$\|H\|_\infty \triangleq \sup_{\mathrm{Re}(s)>0} \|H(s)\|.$$

If H is stable,(i.e., $H \in H_\infty^{p\times q}$), then by the maximum modulus principle, the H_∞-norm reduces to the supremum over the imaginary axis:

$$\|H\|_\infty = \sup_{\omega\in\mathbb{R}} \|H(j\omega)\| = \sup_{\omega>0} \|H(j\omega)\|.$$

In words, the H_∞-norm of a stable transfer function is the peak value of the spectral norm (maximum singular value) of its frequency response over all frequencies.

3 Controller design

3.1 Optimal MIMO PID controller

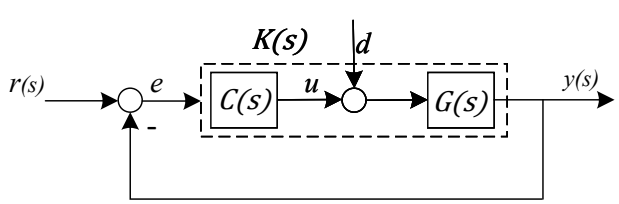

Figure 1: Schematic of the closed-loop feedback interconnection.

The goal of our optimization problem is to minimize the steady-state error. In system Figure 1, with a constant reference, assuming the system is stable and $d = 0$, we have $S(0) = 0$, for sensitivity function, $S(s) = \frac{e(s)}{r(s)} = \big(I + G(s)C(s)\big)^{-1}$. Also, near zero frequency($s \to 0$), $S(s) = s\,(G(0)K_i)^{-1}$. To minimize the steady-state error, we must minimize $\left\|(G(0)K_i)^{-1}\right\|$. Furthermore, we employ few constraints on our problem to achieve better performance. Looking at the feedback system Figure 1, we extract several useful transfer functions for the optimization problem.
Sensitivity function that measures how disturbances and model errors affect the output and should be small for good disturbance rejection and robustness.

$$\|S\|_\infty \le \gamma.$$

Complementary sensitivity function that measures how reference tracking and noise affect the output and should be close to 1 for good tracking, but small at high frequencies for noise rejection.

$$\|T\|_\infty \le \gamma, \quad T = \frac{y}{r} = GC\big(I + GC\big)^{-1},$$

where $\gamma > 1$ and a reasonable range is $1.1 < \gamma < 1.6$.
Control effort transfer function that we want a small control effort to reference tracking.

$$\|Q\|_\infty \le \; Q_{\max}, \quad Q = \frac{u}{r} = C\big(I + GC\big)^{-1}.$$

A reasonable value for $Q_{\max}$ can be determined as follows. Any controller with a finite objective (i.e., perfect reference tracking at $s = 0$) satisfies $T(0) = I = G(0)Q(0)$, meaning that at DC, the controller inverts the plant. This implies $\|Q(0)\| > 1/\sigma_{\min}(G(0))$, and therefore $\|Q\|_\infty > 1/\sigma_{\min}(G(0))$. Hence, we require $Q_{\max} > 1/\sigma_{\min}(G(0))$. The right-hand side is the minimum actuator effort needed for static tracking. So a sensible $Q_{\max}$ is a modest multiple of this value, e.g., 3 to 10. Using the described relations, we first define the optimization problem for a conventional MIMO PID system, and then extend it to a multivariable fuzzy PID control system. The optimization problem for a conventional MIMO PID system is formulated as follows:

$$\begin{array}{ll} \text{Minimize} & \left\|(G(0)K_i)^{-1}\right\| \\ \text{subject to} & \|S\|_\infty \le \gamma \\ & \|T\|_\infty \le \gamma \\ & \|Q\|_\infty \le Q_{\max} \end{array} \tag{6}$$

The constraints of the problem can be written, for example, as follows:

$$\|T(j\omega_k)\|_\infty \le \gamma.$$

This is a semi-infinite constraint, because it consists of an infinite number of constraints for each $\omega_k > 0, \quad k = 1, \ldots, N$. The computational complexity of our optimization method scales linearly with N. Hence, we may select a sufficiently large value of N so that this sampling does not have any practical impact. By "reasonable", we mean that the frequency sampling is sufficiently fine to capture any rapid variations of the closed-loop transfer function with frequency, and that it covers an adequate range. We assume that at ω_1 and ω_N, the transfer functions approach their asymptotic values, for example, considering $T(j\omega_k)$, we obtain:

$$T(0) = I, \quad \textit{and} \quad T(\infty) = 0.$$

The resulting sampled optimization problem can therefore be written as:

$$\begin{array}{ll} \text{Minimize} & \left\|(G(0)K_i)^{-1}\right\| \\ \text{subject to} & \|S_k\|_\infty \le \gamma \\ & \|T_k\|_\infty \le \gamma \\ & \|Q_k\|_\infty \le Q_{\max} \end{array} \quad , k = 1, \ldots, N \tag{7}$$

In the next step, we must transform this norm-constrained problem into an LMI formulation. For details of transforming H_∞-norm constraints into LMIs, see [5, Section 4]:

$$\begin{aligned} &\max\ t \\ &\text{subject to} \quad \begin{bmatrix} F_k^* \tilde{F}_k + \tilde{F}_k^* F_k - \tilde{F}_k^* \tilde{F}_k & Y_k^* \\ Y_k & I \end{bmatrix} \succeq 0, \quad k = 1, \ldots, M, \end{aligned} \tag{8}$$

where t is an auxiliary variable introduced through the epigraph transformation [6, Section 4.2.4]. This is the general form of a convex optimization problem with LMI constraints, where a separate matrix is constructed for each constraint in the form of (8). In this formulation, the term involving $F_k = I + G_k C_k$ is identical for all constraints, whereas the Y_k-dependent part is different for each constraint. For the constraint related to $S(s)$, we have $Y_k = (1/\gamma)I$; for $T(s)$, $Y_k = (1/\gamma)G_k C_k$; and for $Q(s)$, $Y_k = (1/Q_{max})C_k$. Also, $I \in \mathbb{R}^{n\times n}$ is the identity matrix.

Moreover, $\tilde{F}_k$ is a matrix with appropriate dimensions whose value is updated as $\tilde{F}_k = F_k^{curr}$, where F_k^{curr} is the current value of F_k at each iteration. By solving Problem (8) for a MIMO system, the optimal PID controller gains are obtained. In addition, the closed-loop system is guaranteed to be stable.

The next objective is to determine the gains of a multivariable fuzzy PID controller. Suppose the constraints of Problem 8, originally defined for a multivariable system, are now extended to a multivariable fuzzy system. In this case, the number of constraints will depend not only on the number of frequency samples but also on the number of subsystems. Based on the structure and condition of the problem, by solving this, we will also achieve closed-loop stability. Consequently, all subsystems will be asymptotically stable in closed-loop. However, if the final controller obtained for the fuzzy system lies in a decision region that requires the combination of several subsystems, will the system remain stable? The answer will be addressed in the following.

3.2 Optimal MIMO fuzzy PID controller

3.2.1 Takagi-Sugeno fuzzy systems

In a Takagi-Sugeno fuzzy system, rules are defined in the following structure:

$$\text{Fuzzy rule } i: \text{ IF } x_1 \text{ is } M_1^i \text{ and } x_2 \text{ is } M_2^i \text{ and } \ldots \text{ and } x_n \text{ is } M_n^i, \text{ THEN } Y(s) = A_i X + b_i, \quad i = 1, 2, \ldots, r,$$

here, $X = [x_1\ x_2\ \ldots\ x_n]^\top$ is the input vector, and M_l^i denotes the fuzzy set associated with the l-th input variable in the i-th rule. Using a product t-norm for rule activation, a sum s-norm for aggregation, product inference, and weighted-average defuzzification, the system output is given by:

$$Y = \frac{\sum_{i=1}^{r} \mu_i y_i}{\sum_{i=1}^{r} \mu_i}, \tag{9}$$

here, Y is the output of the fuzzy system, y_i is the output of the i-th rule, and μ_i denotes the firing strength (weight) of the i-th rule, which is calculated as:

$$\mu_i = \prod_{l=1}^{n} M_l^i(x). \tag{10}$$

A key advantage of fuzzy systems is that they do not require an exhaustive enumeration of all possible system states in the rule base. For instance, when modeling a nonlinear system, a finite number of linear subsystems can be defined. The fuzzy inference mechanism then interpolates the system behavior in regions that are not explicitly modeled [11].

In a fuzzy system incorporating PID control, the fuzzy rules are formulated as:

$$\text{Rule } i: \text{ IF } x_1 \text{ is } M_1^i \text{ and } x_2 \text{ is } M_2^i \text{ and } \ldots \text{ and } x_n \text{ is } M_n^i, \text{ THEN } Y(s) = U(s)\, G_i(s), \quad i = 1, 2, \ldots, r,$$

here, x_l denotes the l_{th} input, M_l^i represents the membership function of the l_{th} input variable in the i-th rule, and $U(s)G_i(s)$ corresponds to the open-loop transfer function of the i_{th} subsystem. Therefore, we have:

$$Y(s) = \frac{\sum_{i=1}^{r} \mu_i\, U(s) G_i(s)}{\sum_{i=1}^{r} \mu_i}, \tag{11}$$

here, $U(s)$ is the control signal generated by the fuzzy system [14].

$$\text{Rule } j: \text{ IF } x_1 \text{ is } M_1^j \text{ and } x_2 \text{ is } M_2^j \text{ and } \ldots \text{ and } x_n \text{ is } M_n^j, \text{ THEN } U(s) = C_j(s)\, z(s), \quad j = 1, 2, \ldots, r,$$

where $z(s)$ is a combination of the inputs. In this case, we have:

$$U(s) = \frac{\sum_{j=1}^{r} \mu_j \, C_j(s) z(s)}{\sum_{j=1}^{r} \mu_j}. \tag{12}$$

Each of the controller subsystems is represented by a PID controller in the following form:

$$C(s) = \left(K_p + \frac{K_i}{s} + \frac{K_d \, s}{1 + \tau s} \right), \tag{13}$$

where K_p, K_i, and K_d denote the proportional, integral, and derivative gain matrices, respectively, and $\tau > 0$ is the derivative time constant, such that $\frac{1}{\tau s+1}$ acts as a low-pass filter for the derivative action. These matrices are the design parameters to be optimally determined. The overall controller output is:

$$Y = \frac{\sum_{i=1}^{r} \mu_i \left[\sum_{j=1}^{r} \mu_j C_j(s) z(s) \right] G_i(s)}{\sum_{i=1}^{r} \mu_i \sum_{j=1}^{r} \mu_j} = \frac{\sum_{i=1}^{r} \sum_{j=1}^{r} \mu_i \mu_j C_j(s) G_i(s)}{\sum_{i=1}^{r} \sum_{j=1}^{r} \mu_i \mu_j} z(s). \tag{14}$$

In the next section, we describe how to design a fuzzy system based on these relations while guaranteeing closed-loop stability.

3.2.2 Stability of fuzzy system

In this section, the stability of the fuzzy system is analyzed using the Positive Real Lemma. It is shown that a fuzzy system (14) is stable if it satisfies the positive real condition.

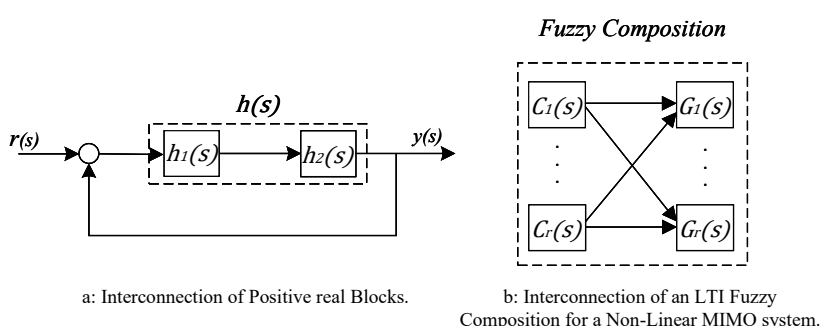

a: Interconnection of Positive real Blocks. b: Interconnection of an LTI Fuzzy Composition for a Non-Linear MIMO system.

Figure 2: Interconnection of a positive real system and the fuzzy composition..

Lemma 3.1. ***(Positive Real)****:*
A MIMO LTI system with transfer function $G(s)$ is Positive Real (PR) if [26]:

1. *$G(s)$ is analytic in* $\mathrm{Re}(s) > 0$ *and any poles on* $\mathrm{Re}(s) = 0$ *are simple.*
2. *For all s with* $\mathrm{Re}(s) > 0$*:*
$$G(s) + G^*(s) \succeq 0,$$
where $G^*(s)$ denotes the conjugate transpose of $G(s)$.
3. *On the imaginary axis ($s = j\omega$):*
$$G(j\omega) + G^*(j\omega) \succeq 0, \quad \forall \omega \in \mathbb{R}.$$

A system is Strictly Positive Real (SPR) if:

1. *$G(s)$ is analytic in* $\mathrm{Re}(s) \geq 0$ *(no poles on the imaginary axis).*

2. *For all* $\omega \in \mathbb{R}$*:*

$$G(j\omega) + G^*(j\omega) \succ 0,$$

i.e., the matrix is positive definite for all real frequencies.

This lemma implies that all poles of the system lie in the left half of the complex plane and based on Parseval's Theorem energy of a Positive real system is finite. Moreover, under this condition, the system is passive and internally stable and Interconnections of positive real blocks in a system with unique feedback remain stable, [7].

Consider a feedback loop with the loop transfer function $h(s) = h_1(s)h_2(s)$, as depicted in Figure 2[a]. If h_1 is passive and h_2 is strictly passive, then the phase angles of these transfer functions satisfy:

$$|\angle h_1(j\omega)| \leq 90^\circ \quad \text{and} \quad |\angle h_2(j\omega)| < 90^\circ.$$

Hence, the phase angle of the loop transfer function $h(s)$ is bounded by:

$$|\angle h(j\omega)| < 180^\circ.$$

Because both h_1 and h_2 are passive (one of them strictly), it follows that $h(s)$ has no poles in the open right-half plane ($\mathrm{Re}[s] > 0$). Therefore, according to the classical Bode–Nyquist stability criterion, the closed-loop system is asymptotically stable as well as BIBO (Bounded-Input Bounded-Output) stable.

Theorem 3.2. ***(Stability of the Fuzzy System):*** *A fuzzy system described by relations(11), (12) and (14) is internally stable if all of its subsystems satisfy the analyticity condition and the following condition holds:*

$$K(j\omega) + K^*(j\omega) \geq 0, \quad \forall\, \omega \geq 0, \tag{15}$$

where $K(j\omega)$ *denotes the open-loop transfer function of the fuzzy system.*

Proof. Using relation (14), the open-loop transfer function of the overall fuzzy system can be written as:

$$K(j\omega) = \frac{\sum_{i=1}^{r}\sum_{j=1}^{r} \mu_i\mu_j\, C_j(j\omega)\, G_i(j\omega)}{\sum_{i=1}^{r}\sum_{j=1}^{r} \mu_i\mu_j} = \sum_{i=1}^{r}\sum_{j=1}^{r} \sigma_{ij}\, C_j(j\omega)\, G_i(j\omega).$$

On the other hand, for the fuzzy system we define normalized weights:

$$\sigma_{ij} \;=\; \frac{(\mu_i\mu_j)}{\sum_{i=1}^{r}\sum_{j=1}^{r} \mu_i\mu_j}, \quad 0 \leq \sigma_{ij} \;\leq 1,$$

such that $\sum_{i,j=1}^{r}(\sigma_{ij}) = 1$, These are inherently positive and real. Therefore, for internal stability of the fuzzy system it suffices to examine:

$$K(j\omega) = C_j(j\omega)\, G_i(j\omega).$$

Then, assuming that the subsystems are stable, we must check the following PR condition to ensure the closed-loop stability of the overall fuzzy control system:

$$\big(C_j(j\omega)\, G_i(j\omega)\big) + \big(C_j(j\omega)\, G_i(j\omega)\big)^* \geq 0. \tag{16}$$

Moreover, a more conservative condition is given by:

$$(C_j(j\omega)G_i(j\omega)) + (C_j(j\omega)G_i(j\omega))^* \geq \varepsilon I, \quad \varepsilon > 0,$$

where ε is a very small real number greater than zero.

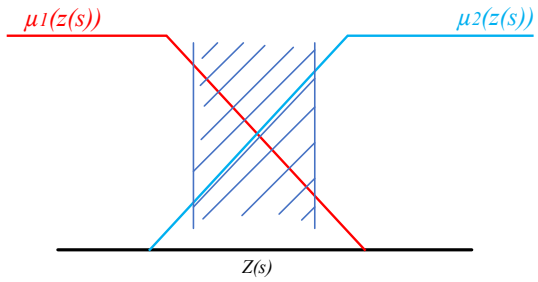

Figure 3: membership functions for a fuzzy composition with two subsystems.

□

In Section 3.1, we stated that Problem (8) alone is not sufficient for the optimal design of a fuzzy system, and additional conditions are required to ensure the stability of the entire fuzzy system. Based on Figure 3, it can be seen that for our optimization problem, only the hatched region will be problematic, while the remaining regions are consistent with Problem (8). To resolve this issue, Condition (16) will be examined for cases where $i \neq j$. This is because the positive real condition is applied to the off-diagonal parts, and in these regions, the system will remain internally stable and closed-loop stable. Based on the relations presented so far, we formulate the overall problem:

$$\begin{aligned} &\max\ t \\ &\text{s.t.} \quad \begin{bmatrix} F(W)_k^* \tilde{F}(W)_k + \tilde{F}(W)_k^* F(W)_k - \tilde{F}(W)_k^* \tilde{F}(W)_k & Y(W)_k^* \\ Y(W)_k & I \end{bmatrix} \succeq 0, \\ &\qquad \big(C_{jk}\, G_{ik}\big) + \big(C_{jk}\, G_{ik}\big)^* \succeq 0, \quad i \neq j, \\ &\qquad k = 1, \ldots, N. \end{aligned} \tag{17}$$

Here, N denotes the number of frequency samples, and W denotes the number of subsystems in the fuzzy system. To formulate Problem (17) for an optimization solver, the objective function and the constraint matrices can be written as:

$$\begin{aligned} &\max \quad t \\ &\text{subject to} \quad \begin{bmatrix} (A(W))_k & 0 & 0 \\ 0 & (B(W))_k & 0 \\ 0 & 0 & (D_{ij})_k \end{bmatrix} \succeq 0. \end{aligned} \tag{18}$$

In this case, we have:

$$A(W) = \begin{bmatrix} F(W)^* \tilde{F}(W) + \tilde{F}(W)^* F(W) - \tilde{F}(W)^* \tilde{F}(W) & Y(W)^* \\ Y(W) & I \end{bmatrix}.$$

This constraint corresponds to the objective of the problem - minimize $\sum_{j=1}^{W} (\left\| (G(0)K_i)^{-1} \right\|)_j$, where each term in the summation is transformed into the problem's constraints using the epigraph transformation.
$B(W)$ represents the constraints imposed on the defined transfer functions, which are given as follows:

$$B(W) = \begin{bmatrix} F(W)^* \tilde{F}(W) + \tilde{F}(W)^* F(W) - \tilde{F}(W)^* \tilde{F}(W) & Y(W)^* \\ Y(W) & I \end{bmatrix}.$$

Also, D_{ij} represents the frequency-domain stability condition of the fuzzy system, defined as:

$$D_{ij} = \big(C_j(j\omega)\, G_i(j\omega)\big) + \big(C_j(j\omega)\, G_i(j\omega)\big)^*.$$

This optimization problem has a linear objective function and LMI constraints. Therefore, it can be solved efficiently while guaranteeing a globally optimal solution.

The general algorithm for the proposed optimization approach is summarized as follows:

Step 1: Linearize the nonlinear system around the operating points and obtain the transfer functions for each subsystem.

Step 2: Initialize the parameters, frequency range, number of frequency samples, and the initial values for γ, τ. The controller parameters are chosen as follows:

$$K_P = 0, \quad K_I = \varepsilon G(0)^+, \quad K_D = 0,$$

where ε is a small positive scalar, and $G(0)^+ = G(0)^T \big(G(0)G(0)^T\big)^{-1}$ denotes the pseudo-inverse of the DC gain.

For a sufficiently small ε, the proposed controller remains feasible. Moreover, as ε approaches zero, we obtain:

$$S(s) \to \frac{s}{s+\varepsilon} I, \quad T(s) \to \frac{\varepsilon}{s+\varepsilon} I, \quad Q(s) \to \frac{\varepsilon}{s+\varepsilon} G(0)^+.$$

From this, it follows that the constraints $\|S\|_\infty \le \gamma$, $\|T\|_\infty \le \gamma$, and $\|Q\|_\infty \le Q_{\max}$ become feasible for a sufficiently small ε (provided that $\gamma > 1$, and $Q_{\max} > \frac{1}{\sigma_{\min}(G(0))}$). It should be noted that a finite $\|Q\|_\infty$ guarantees closed-loop stability for this initial controller.

Step 3: The objective function is transformed into a constraint using the epigraph transformation. A separate epigraph transformation and its corresponding constraint are introduced for each subsystem.

Step 4: Construct the linear matrix inequality (LMI) constraints for every subsystem, together with the overall stability constraint for the fuzzy system.

Afterward, the optimization procedure is executed until the change in the objective value becomes sufficiently small.

4 Examples and simulation

4.1 RR two degrees of freedom robot

The schematic of a two-degree-of-freedom robot Manipulator can be represented as follows:

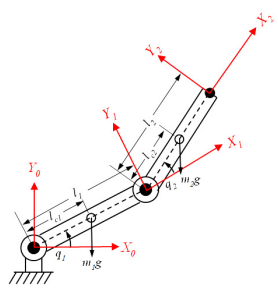

Figure 4: Schematic of a two-degree-of-freedom RR Robot manipulator.

For convenience, the parameters of the robot are defined as follows:

$$l_1 = 1, \quad l_2 = 1, \quad m_1 = 1, \quad m_2 = 1, \quad g = 9.8, \quad I_1 = I_2 = 2.$$

Also, the final dynamic equations of this robot are:

$$
\begin{aligned}
&d_{11}\ddot{q}_1 + d_{12}\ddot{q}_2 + c_{121}\dot{q}_1\dot{q}_2 + c_{211}\dot{q}_2\dot{q}_1 + c_{221}\dot{q}_2^2 + g_1 = \tau_1,\\
&d_{21}\ddot{q}_1 + d_{22}\ddot{q}_2 + c_{112}\dot{q}_1^2 + g_2 = \tau_2,\\
&d_{11} = m_1 l_{c1}^2 + m_2\left(l_1^2 + l_{c2}^2 + 2l_1 l_{c2}\cos q_2\right) + I_1 + I_2,\\
&d_{12} = d_{21} = m_2\left(l_{c2}^2 + l_1 l_{c2}\cos q_2\right) + I_2,\\
&d_{22} = m_2 l_{c2}^2 + I_2,\\
&c_{121} = -m_2 l_1 l_{c2}\sin q_2 = h,\\
&c_{211} = h, \quad c_{221} = h, \quad c_{112} = -h,\\
&g_1 = (m_1 l_{c1} + m_2 l_1)\, g\cos q_1 + m_2 l_{c2} g\cos(q_1 + q_2),\\
&g_2 = m_2 l_{c2} g\cos(q_1 + q_2).
\end{aligned}
$$

To determine the optimal controller parameters, the nonlinear dynamic equations of the system are first linearized about the equilibrium operating points. Since the robot is assumed to move between two operating points, the system is linearized at each of these points. The first operating point corresponds to:

$$[q_1, q_2]_1 = [0.349,\ 0]\ \text{rad},$$

with the corresponding equilibrium control inputs

$$[u_1(0),\ u_2(0)]_1 = [18.41,\ 4.6].$$

The transfer function of the system linearized about this operating point is given by:

$$G_1(s) = \begin{bmatrix} \dfrac{0.70s^4 - 1.56s^2 + 0.77}{2.19s^6 - 8.47s^4 + 10.35s^2 - 3.88} & \dfrac{-0.85s^4 + 1.79s^2 - 0.77}{2.19s^6 - 8.47s^4 + 10.35s^2 - 3.88} \\ \dfrac{-0.57s^2 + 0.35}{1.48s^4 - 3.51s^2 + 1.76} & \dfrac{1.36s^2 - 1.40}{1.48s^4 - 3.51s^2 + 1.76} \end{bmatrix}.$$

The second operating point corresponds to:

$$[q_1, q_2]_2 = [1.483,\ -0.698]\ \text{rad},$$

with the corresponding equilibrium control inputs

$$[u_1(0),\ u_2(0)]_2 = [4.7,\ 3.5].$$

The transfer function of the system linearized about this operating point is given by:

$$G_2(s) = \begin{bmatrix} \dfrac{6.11s^4 - 36.54s^2 + 42.37}{19.47s^6 - 203.28s^4 + 653.96s^2 - 600.48} & \dfrac{-7.15s^4 + 42.49s^2 - 48.16}{19.47s^6 - 203.28s^4 + 653.96s^2 - 600.48} \\ \dfrac{-1.62s^2 + 2.13}{4.14s^4 - 26.59s^2 + 30.83} & \dfrac{3.85s^2 - 11.15}{4.14s^4 - 26.59s^2 + 30.83} \end{bmatrix}.$$

In an optimization problem, we may either consider a set of homogeneous cost functions or define heterogeneous objectives across different subsystems. For instance, one subsystem might require minimization of steady-state error, while another may prioritize overshoot reduction. However, in our problem, the objective is exclusively to minimize the steady-state error in all subsystems.

$$\sum_{j=1}^{W}\left(\left\|\left(G(0)K_i\right)^{-1}\right\|\right)_j, \quad W = 2,$$

where the Matrices of the transfer function in the steady state are:

$$G_1(0) = \begin{bmatrix} -0.1989 & 0.1989 \\ 0.1989 & -0.7957 \end{bmatrix}, \quad G_2(0) = \begin{bmatrix} -0.0706 & 0.0802 \\ 0.0692 & -0.3616 \end{bmatrix}.$$

The values of the initial parameters to implement the optimization method for all subsystems are selected as follows, the value of τ can be selected for each subsystem separately:

$$\varepsilon = 0.5, \quad \tau_1 = 4, \quad \tau_2 = 6, \quad \gamma = 1.4,$$
$$Q_1\max = Q_2\max > \frac{3}{\sigma_{\min}(G(0))} = 100.$$

These values are selected according to the conditions and dynamics of the system.

The number of samples is $N = 50$, logarithmically distributed in the interval $[10^{-3}, 10^3]$. The number of samples and their definition interval are selected according to the dynamics and working conditions of the system; robot manipulators usually represent systems that do not undergo rapid changes. Consequently, a reduced number of samples is utilized in our optimization algorithm. For optimization, SDPT3 software [19, 23] and the CVX program, which is based on MATLAB [1, 10], have been used. CVX is a MATLAB toolbox for specifying and solving convex optimization problems, including LMIs, linear programming, and quadratic programming. Using a natural, mathematical syntax, it automatically verifies problem convexity and interfaces with efficient solvers. In control engineering, CVX is commonly employed for Lyapunov-based stability analysis, H∞ controller synthesis, and semidefinite programming formulations, though it is restricted to convex problems and offline design. The general structure of the problem for optimizing this system is:

$$\begin{aligned} &\min \quad \left\| \left(G_1(0)K_{i1}\right)^{-1} \right\| + \left\| \left(G_2(0)K_{i2}\right)^{-1} \right\| \\ &\text{subject to} \begin{bmatrix} B(1)_k & 0 & 0 & 0 \\ 0 & B(2)_k & 0 & 0 \\ 0 & 0 & \left(D_{12}\right)_k & 0 \\ 0 & 0 & 0 & \left(D_{21}\right)_k \end{bmatrix} \succeq 0, \end{aligned}$$

where the matrices $B(1)$ and $B(2)$ are written as:

$$B(1) = \begin{bmatrix} F(1)^*\tilde{F}(1) + \tilde{F}(1)^*F(1) - \tilde{F}(1)^*\tilde{F}(1) & Y(1)^* \\ Y(1) & I \end{bmatrix},$$

$$B(2) = \begin{bmatrix} F(2)^*\tilde{F}(2) + \tilde{F}(2)^*F(2) - \tilde{F}(2)^*\tilde{F}(2) & Y(2)^* \\ Y(2) & I \end{bmatrix},$$

where $F(1) = I + G_1C_1$ and $\tilde{F}(1) = I + G_1(0)C_1(0)$, which is substituted into $F(1)^{curr}$ at each iteration. The parameters for the second subsystem are the same. As mentioned, F is the same for all constraints (S, T, Q) of each subsystem, while Y is different.

After reformulating the objective function as a constraint using the epigraph transformation, the optimization problem takes the following form:

$$\begin{aligned} &\min \quad t \\ &\text{subject to} \begin{bmatrix} A(1) & 0 & 0 & 0 & 0 & 0 \\ 0 & A(2) & 0 & 0 & 0 & 0 \\ 0 & 0 & B(1)_k & 0 & 0 & 0 \\ 0 & 0 & 0 & B(2)_k & 0 & 0 \\ 0 & 0 & 0 & 0 & \left(C_{1k}G_{2k}\right) + \left(C_{1k}G_{2k}\right)^* & 0 \\ 0 & 0 & 0 & 0 & 0 & \left(C_{2k}G_{1k}\right) + \left(C_{2k}G_{1k}\right)^* \end{bmatrix} \succeq 0. \end{aligned}$$

The matrix $A(1)$ is:

$$A(1) = \begin{bmatrix} F(1)^*\tilde{F}(1) + \tilde{F}(1)^*F(1) - \tilde{F}(1)^*\tilde{F}(1) & Y(1)^* \\ Y(1) & I \end{bmatrix}.$$

So we have:

$$F(1) = G_1(0)K_{i1}, \quad \tilde{F}(1) = G_1(0)K_{i1}(0), \quad Y(1) = tI.$$

Note that $K_{i1}(0)$ is the initial value of the integrator matrix. The relationship for $A(2)$ is similar.

After the configuration of the problem is completed, the algorithm is executed, and the following matrices for the controller are obtained.

$$K_{p1} = \begin{bmatrix} -30.9851 & -11.0249 \\ -7.9853 & -8.9729 \end{bmatrix}, \quad K_{i1} = \begin{bmatrix} -11.1176 & -2.9692 \\ -2.7459 & -2.8351 \end{bmatrix}, \quad K_{d1} = \begin{bmatrix} -23.7747 & -14.8532 \\ -5.5292 & -9.1105 \end{bmatrix},$$

$$K_{p2} = \begin{bmatrix} -77.7915 & -23.5802 \\ -15.1083 & -17.2995 \end{bmatrix}, \quad K_{i2} = \begin{bmatrix} -30.0470 & -7.1723 \\ -5.6736 & -5.9776 \end{bmatrix}, \quad K_{d2} = \begin{bmatrix} -44.1858 & -26.4166 \\ -7.5757 & -13.6186 \end{bmatrix}.$$

The optimal value of the objective function has been obtained $\sum_{j=1}^{2}(\left\|\left(G(0)K_i\right)^{-1}\right\|)_j = 1.2$. Figure 5, shows the positivity condition of fuzzy system over the frequency interval.

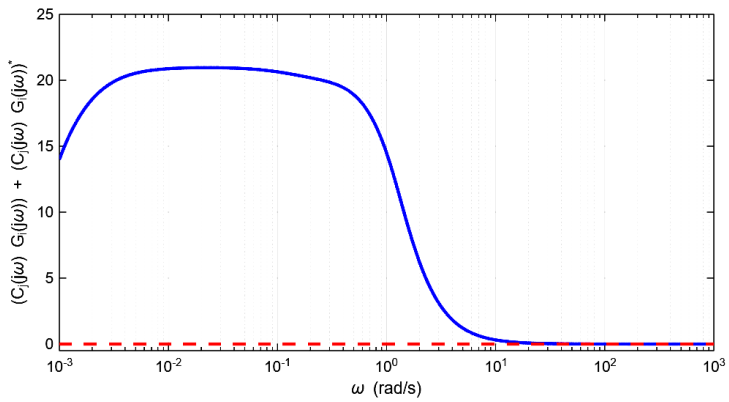

Figure 5: Positive real condition of the fuzzy system over the frequency range..

The control objective is to ensure that the system output accurately tracks the reference signal. Accordingly, based on the system output, the fuzzy controller determines the contribution (weighting factor) of each subsystem in generating the control signal. To this end, the first system output, q_1, is selected as the fuzzy controller's premise variable. This choice is made for the sake of simplicity. Since the system consists of two subsystems and the fuzzy controller is designed to provide a smooth transition between their corresponding operating regions, the membership functions shown below are employed. The system outputs serve as premise variables in the fuzzy inference mechanism, whereas the control signal is generated based on the tracking error.

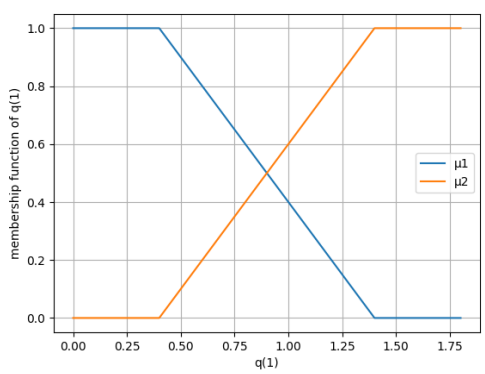

Figure 6: Membership functions of q(1).

The fuzzy rules must be defined to cover all subsystems and operating points of the robot. Since our system is defined in two regions, the fuzzy rules are formulated in the following form:

R1) If q_1 is about 0.349, then $U = K_{p1}E + K_{i1}IE + K_{d1}DE + u_1(0)$.

R2) If q_1 is about 1.483, then $U = K_{p2}E + K_{i2}IE + K_{d2}DE + u_2(0)$.

where E is the error vector input to the fuzzy system, IE is the integral of the error vector, and DE is the derivative of the error vector. The constant values u_1 and u_2 represent the equilibrium points of the control signal.

To better evaluate the MFP controller, it is compared with two other methods: the Adaptive Fuzzy (AF) controller [8], and the Integral Terminal Sliding Mode Controller(ITSM)[20].

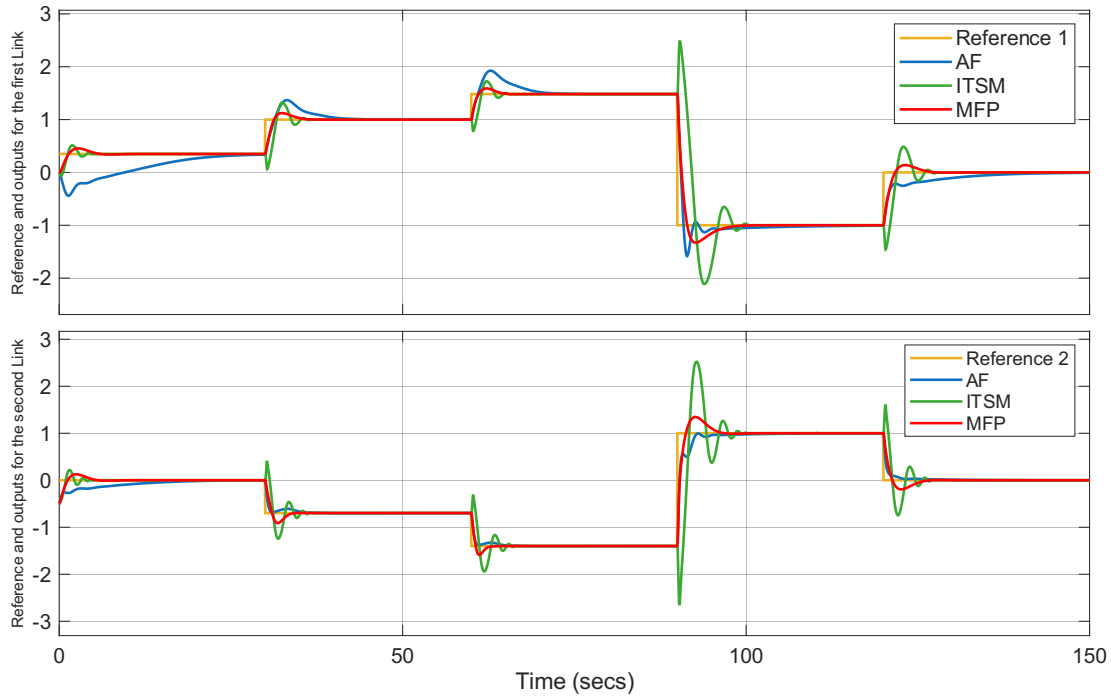

Figure 7: Comparison of reference tracking performance for the MFP, ITSM, and AF controllers.

In the two tables below, we examine and compare the overshoot, settling time, rise time, and IAE(Integral of Absolute Error) for the two robot links.

Table 1: Link 1

Control Method	**Parameter**	**Overshoot (%)**	**Rise Time (s)**	**Settling Time (s)**	**IAE**
MFP	Min	5	0.5	4	
	Max	12	1.2	7	5.31
ITSM	Min	6	0.8	3.5	
	Max	44	1.5	10	14.20
AF	Min	0	0.4	7	
	Max	96	21	25	17.07

Table 2: Link 2

Control Method	**Parameter**	**Overshoot (%)**	**Rise Time (s)**	**Settling Time (s)**	**IAE**
MFP	Min	3	0.6	3	
	Max	10	1.4	7	4.71
ITSM	Min	4	0.5	3	
	Max	68	1.7	11	13.72
AF	Min	0	0.5	2.5	
	Max	0	11	13	5.86

As can be observed, the system output can track the reference input. Moreover, it is clearly evident that the proposed

controller exhibits satisfactory performance. The tables parametrically compare the performance of the three controllers. Moreover, we have the control signals:

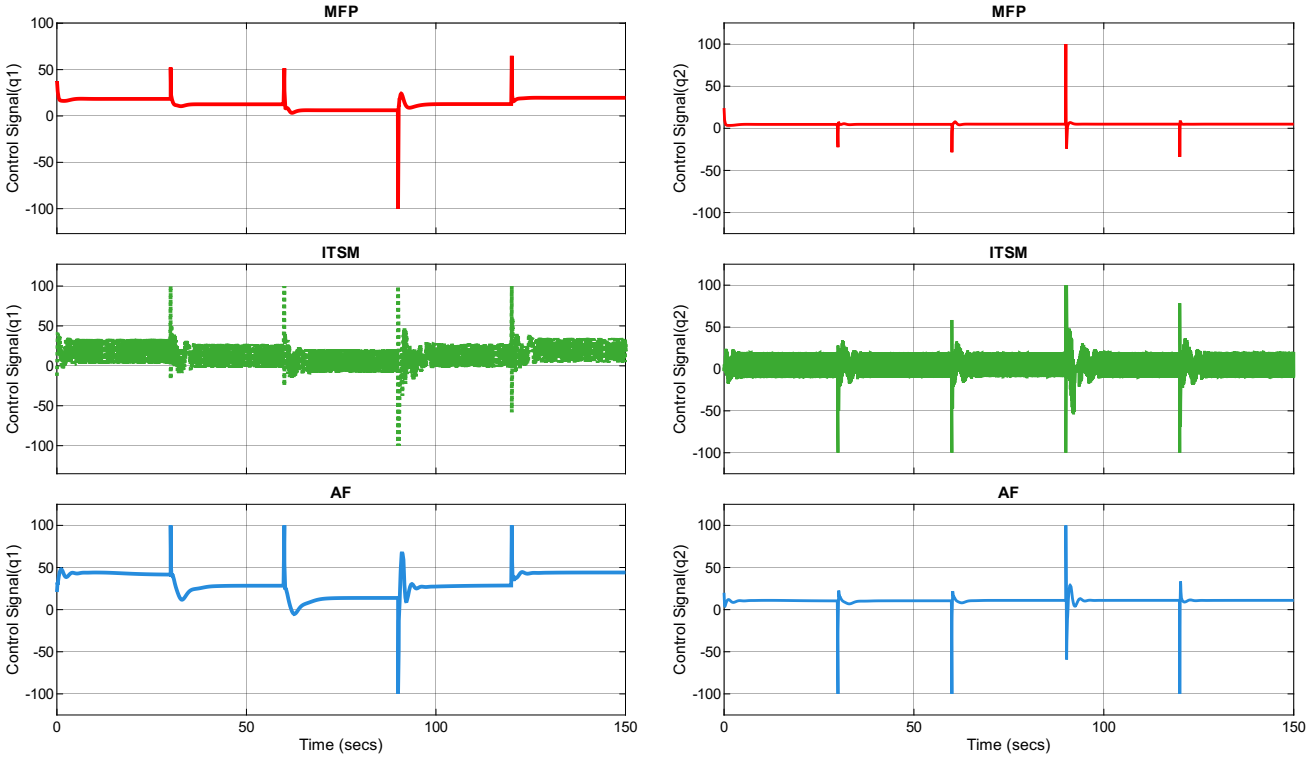

Figure 8: Control signals of the robot manipulator under the MFP, ITSM, and AF controllers.

Based on the control signals generated by the three controllers, it can be observed that the proposed MFP controller regulates the system using a smaller control range and lower control effort. In contrast, the adaptive fuzzy controller generates significantly larger control signals in response to abrupt changes in the system. Furthermore, the sliding mode controller exhibits considerable fluctuations in the control signal.

4.2 Mentor's five degrees of freedom robot

Figure 9: Five degrees of freedom mentor Robot [2].

The 5-DOF Mentor robot is an educational and research robot used for simulating and controlling industrial-like manipulators [2]. This robot features 5 Degrees of Freedom (DOF), typically consisting of the following joints: Waist: Rotation about the vertical axis. Shoulder and Elbow: Motion in the vertical plane. Wrist: Usually 2 or 3 final DOF for

tool orientation and rotation. This configuration allows the robot to move within a spherical or cylindrical workspace, similar to many small and medium-sized industrial robots. The Mentor robot employs 24-volt DC motors coupled with gearboxes for each joint, resulting in relatively slow motion. Angular positions are measured using potentiometers. The dynamic model of the robot does not explicitly include gearbox effects (e.g., friction, backlash); this simplification is warranted by the slow operating speed and inherent stiffness of the gearbox. For the sake of simplicity, only two links-namely the shoulder and the forearm-are used. In this case, the setup is similar to the previous example, but with different parameters. Since the dynamic equations of the robot are not available, the mass and inertia tensors are estimated approximately. The estimated weight of each arm is considered to be 6 kilograms, with the shoulder length set to 33 centimeters and the forearm length to 30 centimeters. The inertia tensors are also calculated in unit form. The motion of these two links is initiated from an initial position in the first quadrant, characterized by the following specifications:

$$[q_1, q_2]_1 = [0.2,\ 0.2] \quad \text{rad.}$$

In this case,we have the transfer function $G_1(s)$:

$$G_1(s) = \begin{bmatrix} \dfrac{2.23s^4 - 9.37s^2 + 9.5}{6.24s^6 - 43.19s^4 + 98.57s^2 - 73.41} & \dfrac{-2.53s^4 + 9.94s^2 - 9.05}{6.24s^6 - 43.19s^4 + 98.57s^2 - 73.41} \\ \dfrac{-1.01s^2 + 1.84}{2.49s^4 - 11.13s^2 + 11.83} & \dfrac{2.32s^2 - 5}{2.49s^4 - 11.13s^2 + 11.83} \end{bmatrix}.$$

Also, for the second region at the point $[q_1, q_2]_2 = [1.4,\ -0.7]$rad, the $G_2(s)$ is:

$$G_2(s) = \begin{bmatrix} \dfrac{36.99s^4 - 476s^2 + 1023}{103s^6 - 2382s^4 + 16382s^2 - 29033} & \dfrac{-40.63s^4 + 525s^2 - 1138}{103s^6 - 2382s^4 + 16382s^2 - 29033} \\ \dfrac{-3.99s^2 + 9.65}{10.16s^4 - 130s^2 + 280} & \dfrac{9.15s^2 - 59.05}{10.16s^4 - 130s^2 + 280} \end{bmatrix}.$$

The equilibrium values of the control signal are calculated as $U_1(0) = [-0.8,\ -0.2]$ and $U_2(0) = [-8.5,\ -13.8]$. The steady-state transfer function matrix is:

$$G_1(0) = \begin{bmatrix} -0.1294 & 0.1234 \\ 0.1555 & -0.4225 \end{bmatrix}, \quad G_2(0) = \begin{bmatrix} -0.0353 & 0.0392 \\ 0.0344 & -0.2104 \end{bmatrix}.$$

Fuzzy rules and membership functions are defined in the same manner as in the previous example. The initial parameter values for the system are as follows:

$$\varepsilon = 0.3, \quad \tau_1 = \tau_2 = 0.5, \quad \gamma = 1.4,$$
$$Q_1\max = Q_2\max > \frac{1}{\sigma_{\min}(G(0))} = 35.$$

The number of samples is also $N = 50$ logarithmically in the interval $[10^{-3}, 10^3]$. Fuzzy membership functions are defined as in the previous example.

To optimize the controller values of each subsystem, the proposed method is used and the following results are obtained:

$$K_{p1} = \begin{bmatrix} -21.6343 & -16.7611 \\ -7.5089 & -13.6057 \end{bmatrix}, \quad K_{i1} = \begin{bmatrix} -7.4098 & 1.7649 \\ -2.8759 & -0.4887 \end{bmatrix}, \quad K_{d1} = \begin{bmatrix} 7.1106 & 8.9206 \\ 4.1142 & 2.2176 \end{bmatrix},$$

$$K_{p2} = \begin{bmatrix} -50.4542 & -4.9472 \\ -3.3207 & -18.2968 \end{bmatrix}, \quad K_{i2} = \begin{bmatrix} -10.2655 & -2.7351 \\ -0.9862 & -5.2298 \end{bmatrix}, \quad K_{d2} = \begin{bmatrix} 13.3574 & 2.7136 \\ 1.2889 & -1.7221 \end{bmatrix}.$$

The optimal value in this case is 5.0827.

To control the robot, bidirectional communication must be established between the PC (running MATLAB) and the robot. The control signal computed in MATLAB is transmitted to the robot through a communication interface. Likewise, the positions of the robot joints, measured by the position sensors, are sent back to the PC through the same interface. The following embedded interface board manages all communication between the laptop and the robot.

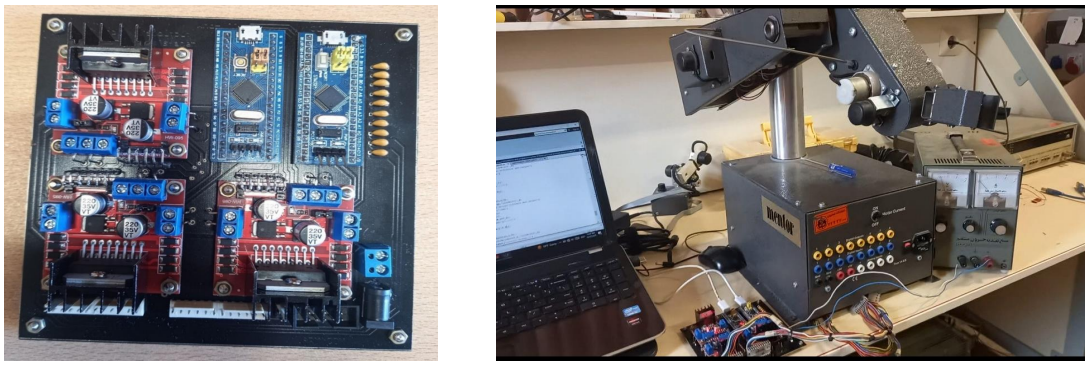

a: interface board for communication between mentor robot and PC.

b: Practical implementation of a multivariable fuzzy PID controller for the Mentor robot

Figure 10: Embedded interface board for communication between the robot and the PC, and practical implementation of the Mentor robot.

This embedded board utilizes two ARM-based STM32 microcontrollers. One microcontroller is responsible for transmitting data from the robot to the PC, while the other handles data transmission from the PC to the robot. Bidirectional communication is established through a USB interface. L298 driver modules are employed to amplify the output signals of the microcontrollers. The microcontrollers are programmed in the C programming language using the KEIL development environment. The main board was designed using Altium Designer. Through this embedded board, the controller designed in MATLAB can be effectively implemented to control the robot.

The controller designed in MATLAB is implemented in discrete time with a sampling period of $t_s = 0.1\,\mathrm{s}$. The discrete-time controllers corresponding to each subsystem of the fuzzy system are given as follows:

$$u_i[n] = K_{P_i} E[n] + K_{I_i} \left(E[n] + E[n-1]\right) t_s + K_{D_i} \frac{E[n] - E[n-1]}{t_s}.$$

The following figures illustrate the experimental performance of the robot when a 0.5 kg load was attached to its gripper.

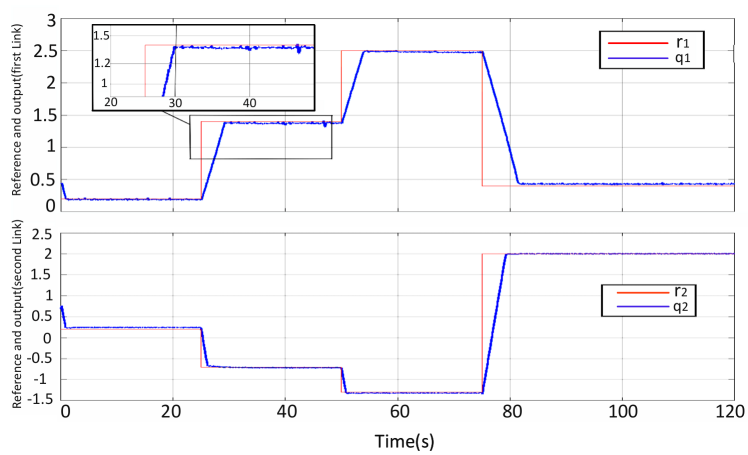

Figure 11: Position responses of the two links to the reference signal.

The small ripples observed in the robot output are caused by noise in the analog-to-digital converters (ADCs) of the STM32 microcontrollers. Considering the voltage limits of the DC motors driving the robot arm, denoted by $u_{\min}$ and $u_{\max}$, the robot output exhibits neither overshoot nor a long settling time.

Likewise, the corresponding control signals are shown below:

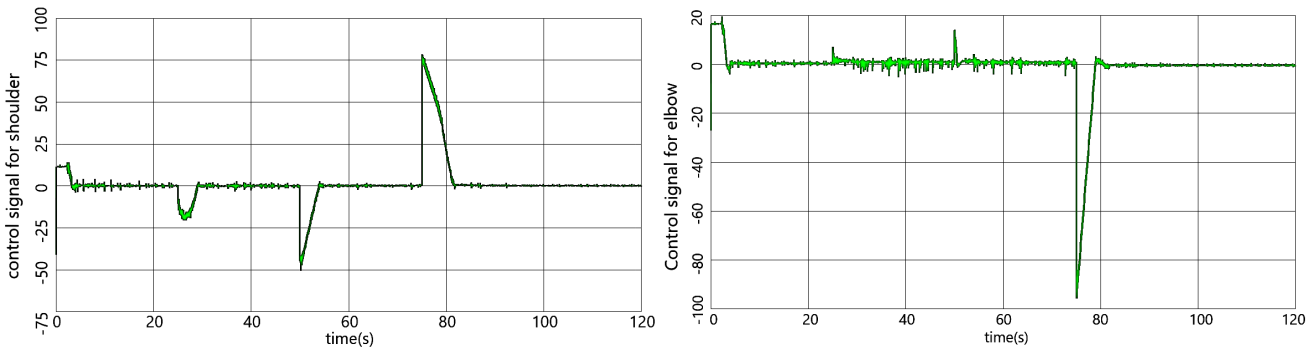

a) Control signal applied to first link

b) Control signal applied to second link

Figure 12: Control signals applied to the Mentor robot manipulator in the practical experiment.

According to the experimental results, the system output successfully tracks the reference input. In this experiment, the robot's gripper carries a 0.5 kg payload, demonstrating the robustness of the proposed control system. The robot is equipped with a gearbox that prevents motion when the control signal is zero. Consequently, the control signal varies only in response to changes in the tracking error, and as the robot reaches the desired position, the control signal converges to zero.

4.2.1 Controller in diagonal mode

The controller analyzed in the previous section was designed in a centralized control framework, where all elements of the controller matrix contain nonzero values. While centralized control offers certain advantages, it also presents several drawbacks, such as higher maintenance costs and increased complexity compared to decentralized control. Moreover, a failure in a single sensor may lead to system instability and potential damage. Therefore, in many cases, control loops are designed independently, resembling single-input single-output (SISO) loops. In this context, we will obtain a diagonal controller; the following results are obtained. The initial parameters for the algorithm are the same as those used in the previous example).

$$K_{p1} = \begin{bmatrix} -11.7448 & 0 \\ 0 & -13.0198 \end{bmatrix}, \quad K_{i1} = \begin{bmatrix} -1.8054 & 0 \\ 0 & -2.7636 \end{bmatrix}, \quad K_{d1} = \begin{bmatrix} 0.8969 & 0 \\ 0 & -5.0841 \end{bmatrix},$$

$$K_{p2} = \begin{bmatrix} -44.6430 & 0 \\ 0 & -24.4444 \end{bmatrix}, \quad K_{i2} = \begin{bmatrix} -7.7804 & 0 \\ 0 & -5.9269 \end{bmatrix}, \quad K_{d2} = \begin{bmatrix} 0.8431 & 0 \\ 0 & -9.1895 \end{bmatrix}.$$

The optimal value is 10.1713.

The results obtained from the robot with half a kilogram of weight in the gripper are as follows:

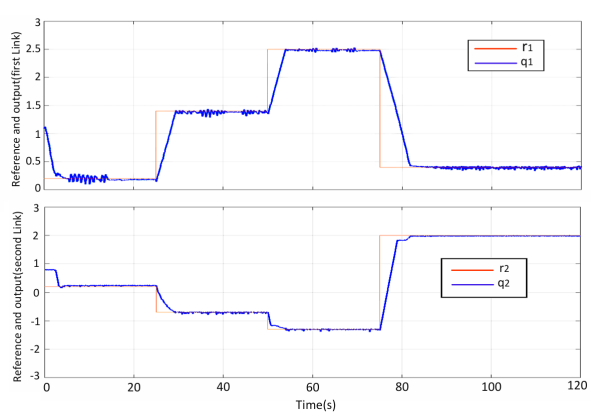

Figure 13: Position responses of the two robot links to the reference signal in the practical implementation of the Mentor robot manipulator using the decentralized controller.

The results for the diagonal controller also show the efficiency of the MFP controller.

5 Conclusion

One of the main challenges faced by control engineers is the control of multivariable systems. Numerous methods have been proposed to address this issue; however, each comes with its own limitations that must be overcome. Among these methods, LMI-based optimization has been effectively applied to linear multivariable systems. Nevertheless, it is generally not applicable to nonlinear systems. In this paper, we employ LMI-based optimization in the frequency domain for nonlinear multivariable systems. The proposed controller is a multivariable fuzzy PID controller using convex optimization. We were able to obtain optimal values for the fuzzy PID control subsystems, whereas normally obtaining this many parameters for optimal system performance is difficult. On the other hand, by using the positive real condition, we achieved stability of the overall system. We demonstrate that by incorporating appropriate LMI constraints into the optimization problem, the optimal solution guarantees both system performance and stability. The effectiveness of the proposed controller is validated through two case studies: one via simulation and the other through practical implementation. Furthermore, in the practical example, we attached a weight of 0.5 kg to the end of the second link, and on the other hand, we modeled the robot without knowing its exact parameters. Our controller effectively, controlled the robot despite these uncertainties.

References

[1] A. Agrawal, R. Verschueren, S. Diamond, S. P. Boyd, *A rewriting system for convex optimization problems*, Journal of Control and Decision, **5**(1) (2018), 42-60. https://doi.org/10.1080/23307706.2017.1397554

[2] R. T. Bambang, *Development of architectures for internet telerobotics systems*, Journal of Bionic Engineering, **4**(4) (2007), 291-297. https://doi.org/10.1016/S1672-6529(07)60043-2

[3] R. P. Borase, D. K. Maghade, S. Y. Sondkar, S. N. Pawar, *A review of PID control, tuning methods and applications*, International Journal of Dynamics and Control, **9**(2) (2021), 818-827. https://doi.org/10.1007/s40435-020-00665-4

[4] M. Boreale, L. Collodi, *Linearization, model reduction and reachability in nonlinear ODEs*, Formal Methods in System Design, **66** (2025), 419-454. https://doi.org/10.1007/s10703-025-00477-2

[5] S. Boyd, M. Hast, K. J. Åström, *MIMO PID tuning via iterated LMI restriction*, International Journal of Robust and Nonlinear Control, **26**(8) (2016), 1718-1731. https://doi.org/10.1002/rnc.3376

[6] S. Boyd, L. Vandenberghe, *Convex optimization*, Cambridge University Press, Cambridge, UK, (2004), 142-144. https://doi.org/10.1017/CBO9780511804441

[7] B. Brogliato, R. Lozano, B. Maschke, O. Egeland, *Dissipative systems analysis and control: Theory and applications*, 3rd ed., Springer, Cham, (2020), 7-38. https://doi.org/10.1007/978-3-030-19420-8

[8] S. Fateh, M. M. Fateh, *Adaptive fuzzy control of robot manipulators with asymptotic tracking performance*, Journal of Control, Automation and Electrical Systems, **31** (2020), 52-61. https://doi.org/10.1007/s40313-019-00496-5

[9] D. Gontijo, J. M. Araújo, F. O. Souza, *Robust multivariable PID controller design for MIMO second order systems: A linear matrix inequality approach*, Proceedings of the Institution of Mechanical Engineers, Part I: Journal of Systems and Control Engineering, **239**(5) (2025), 870-880. https://doi.org/10.1177/09596518241300677

[10] M. C. Grant, S. P. Boyd, *Graph implementations for nonsmooth convex programs*, in Recent Advances in Learning and Control, Springer, (2008), 95-110. https://doi.org/10.1007/978-1-84800-155-8_7

[11] B. Kosko, *Fuzzy systems as universal approximators*, IEEE Transactions on Computers, **43**(11) (1994), 1329-1333. https://doi.org/10.1109/12.324566

[12] Q. Li, X. Zhou, F. Lin, et al., *Novel proportional-integral-derivative control framework on continuous-time positive systems using linear programming*, Mathematics, **12**(4) (2024), 617. https://doi.org/10.3390/math12040617

[13] T. M. Linhares, E. S. Tognetti, T. R. Calliero, *Output feedback control with inexact premise variables of T-S fuzzy systems*, IEEE Transactions on Systems, Man, and Cybernetics: Systems, **55**(3) (2025), 2380-2386. https://doi.org/10.1109/TSMC.2024.3521369

[14] J. Liu, *Intelligent control design and MATLAB simulation*, Springer, Singapore, (2017), 60-65. https://doi.org/10.1007/978-981-10-5263-7

[15] J. Luo, J. Li, L. Xiao, et al., *A novel proportional-integral-parameter zeroing neural network and its application to the quaternion-valued time-varying linear matrix inequality*, IEEE Transactions on Emerging Topics in Computing, **13**(4) (2025), 1565-1576. https://doi.org/10.1109/TETC.2025.3629357

[16] L. A. Mozelli, V. C. da S. Campos, *An improved control law for TS fuzzy models: Less conservative LMI conditions by using membership functions derivative*, Fuzzy Sets and Systems, **517** (2025), 109455. https://doi.org/10.1016/j.fss.2025.109455

[17] Y. Quilles-Marinho, R. C. L. F. Oliveira, P. L. D. Peres, *Output-feedback control design for Takagi-Sugeno fuzzy systems through Lyapunov functions depending polynomially on the states*, Fuzzy Sets and Systems, **499** (2025), 109156. https://doi.org/10.1016/j.fss.2024.109156

[18] R. Sanchis, I. Peñarrocha, *A PID tuning approach to find the optimal compromise among robustness, performance and control effort: Implementation in a free software tool*, International Journal of Control, **97**(1) (2024), 16-35. https://doi.org/10.1080/00207179.2021.1989491

[19] J. F. Sturm, *Using SeDuMi 1.02, a MATLAB toolbox for optimization over symmetric cones*, Optimization Methods and Software, **11**(1-4) (1999), 625-653. https://doi.org/10.1080/10556789908805766

[20] Y. Su, C. Zheng, *A new nonsingular integral terminal sliding mode control for robot manipulators*, International Journal of Systems Science, **51**(8) (2020), 1418-1428. https://doi.org/10.1080/00207721.2020.1764658

[21] H. H. Tang, N. S. Ahmad, *Fuzzy logic approach for controlling uncertain and nonlinear systems: A comprehensive review of applications and advances*, Systems Science and Control Engineering, **12**(1) (2024), 2394429. https://doi.org/10.1080/21642583.2024.2394429

[22] V. Tinoco, M. F. Silva, F. N. Santos, et al., *A review of advanced controller methodologies for robotic manipulators*, International Journal of Dynamics and Control, **13** (2025), 36. https://doi.org/10.1007/s40435-024-01533-1

[23] R. H. Tütüncü, K. C. Toh, M. J. Todd, *Solving semidefinite-quadratic-linear programs using SDPT3*, Mathematical Programming, **95** (2003), 189-217. https://doi.org/10.1007/s10107-002-0347-5

[24] H. F. Yamanaka, D. J. S. Oncoy, R. Cardim, et al., *Robust control with feedback of positions for nonlinear mechanical systems represented by fuzzy T-S models*, in Proceedings of the Brazilian Congress of Automation (CBA 2024), (2024). https://doi.org/10.20906/CBA2024/4413

[25] J. F. Zhang, J. W. Wang, H. K. Lam, H. X. Li, *Boundary output tracking of nonlinear parabolic differential systems via fuzzy PID control*, IEEE Transactions on Fuzzy Systems, **32**(12) (2024), 6863-6877. https://doi.org/10.1109/TFUZZ.2024.3432554

[26] Y. Zhu, R. Chen, S. Xiao, et al., *Positive real lemmas for singular fractional order systems without equality constraints*, Advances in Guidance, Navigation and Control, Lecture Notes in Electrical Engineering, **1349**, Springer, Singapore, (2025), 474-482. https://doi.org/10.1007/978-981-96-2248-1_46